ACS APPLIED MATERIALS & INTERFACES

Research Article

www.acsami.org

Catalyst-Free Cycloaddition Reaction for the Synthesis of Glyconanoparticles

Na Kong,[†] Sheng Xie,[†] Juan Zhou,[†] Margarita Menéndez,[‡] Dolores Solís,[‡] JaeHyeung Park,[§] Giampiero Proietti,[†] Olof Ramström,*[,†] and Mingdi Yan*[,†,§]

[†]Department of Chemistry, KTH-Royal Institute of Technology, Teknikringen 30, S-10044 Stockholm, Sweden

[‡]Consejo Superior de Investigaciones Científicas, and Centro de Investigación Biomédica en Red de Enfermedades Respiratorias (CIBERES), ISCIII, Instituto de Química Física Rocasolano, Madrid, Spain

[§]Department of Chemistry, University of Massachusetts Lowell, 1 University Avenue, Lowell, Massachusetts 01854, United States

Supporting Information

ABSTRACT: A new conjugation method for the immobilization of carbohydrates on nanomaterials was demonstrated simply by mixing perfluorophenyl azide-functionalized silica nanoparticles (SNPs), an amine-derivatized carbohydrate, and phenylacetaldehyde under ambient conditions without any catalyst. The density of carbohydrates on the glyconanoparticles was determined using the quantitative ^{19}F NMR technique; for example, the density of D-mannose (Man) on Man-SNPs was $2.5 \pm 0.2 \times 10^{-16}$ nmol/nm^2. The glyconanoparticles retained their binding affinity and selectivity toward cognate lectins. The apparent dissociation constant of the glyconanoparticles was measured by a fluorescence competition assay, where the binding affinity of Man-SNPs was almost 4 orders of magnitude higher than that of Man with concanavalin A. Moreover, even with a ligand density of 2.6 times lower than Man-SNPs synthesized by the copper-catalyzed azide−alkyne cycloaddition, the binding affinity of Man-SNPs prepared by the current method was more than 4 times higher.

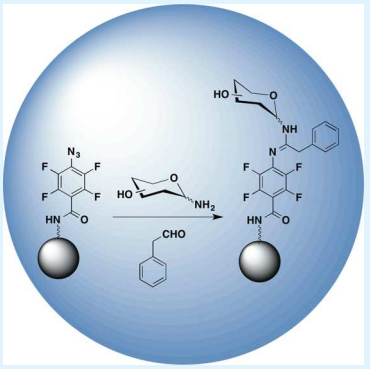

KEYWORDS: *carbohydrates, glyconanomaterials, coupling chemistry, perfluoroaryl azides, ^{19}F qNMR*

INTRODUCTION

Carbohydrates, one of the most structurally complex classes of biomolecules, mediate many biological processes, such as apoptosis, bacterial and viral infections, and immune responses. In addition to their structural complexity, carbohydrates suffer from weak binding affinities toward their cognate receptors. Glyconanomaterials use nanomaterials as scaffolds to multivalently present carbohydrate ligands, thereby increasing the binding affinity toward the respective receptors.[1−3] In addition, the nanoscale size and the unique electronic, optical, and mechanical properties of nanomaterials render the glyconanomaterials attractive for biosensing, bioimaging, and therapeutics.[1,2,4−9] For example, we have recently shown that glyconanomaterials can selectively target different bacteria[10−12] and increase the antibacterial activities of antibiotics.[13−15]

A number of coupling chemistries have been applied to synthesize glyconanomaterials,[1,2,4,5,16] of which the click chemistry has gained increasing popularity, partly owing to the high tolerance of the azide functionality to numerous organic conditions and biological environments. For example, glyconanomaterials have been synthesized by the copper-catalyzed azide−alkyne cycloaddition (CuAAC),[17−23] strain-promoted azide−alkyne cycloaddition (SPAAC),[24−26] and the Staudinger ligation.[27] Among these, CuAAC has the advantages of relatively mild reaction conditions and favorable kinetics. However, CuAAC has its limitations, especially for in vivo applications, due to the possible cytotoxicity of the copper catalyst to biomolecules and living cells.[28−30] SPAAC eliminates the use of the copper catalyst by employing ring strain-activated cyclooctynes but suffers from the relative complex synthesis of cyclooctyne derivatives.[31] In Staudinger ligation, phosphine oxide byproducts are often formed from the oxidation of phosphines, which readily occurs under ambient conditions.[32]

Recently, we have developed a series of reactions using electrophilically activated azides, perfluoroaryl azides (PFAAs).[33−36] The highly electronegative F atoms lower the lowest unoccupied molecular orbital (LUMO) of the PFAAs,[33] accelerate their reactions with dipolarophiles and nucleophiles, and allow the reactions to be carried out under mild conditions without the use of any metal catalyst. In one example, PFAA reacts readily with enamines at room temperature to give amidines in high yields.[33] Inspired by this reaction, we designed a protocol to conjugate carbohydrates to nanoparticles using perfluorophenyl azide-functionalized silica nanoparticles (PFPA-SNPs). To further simplify the protocol, enamines were formed in situ from carbohydrate amines and phenylacetaldehyde. A quantitative fluorine nuclear magnetic resonance spectroscopy (^{19}F qNMR) method was applied to

Received: June 20, 2016
Accepted: September 21, 2016

DOI: 10.1021/acsami.6b07471
ACS Appl. Mater. Interfaces XXXX, XXX, XXX−XXX

Scheme 1. Synthesis of (A) Model Compound 2 and (B) Man-SNPs

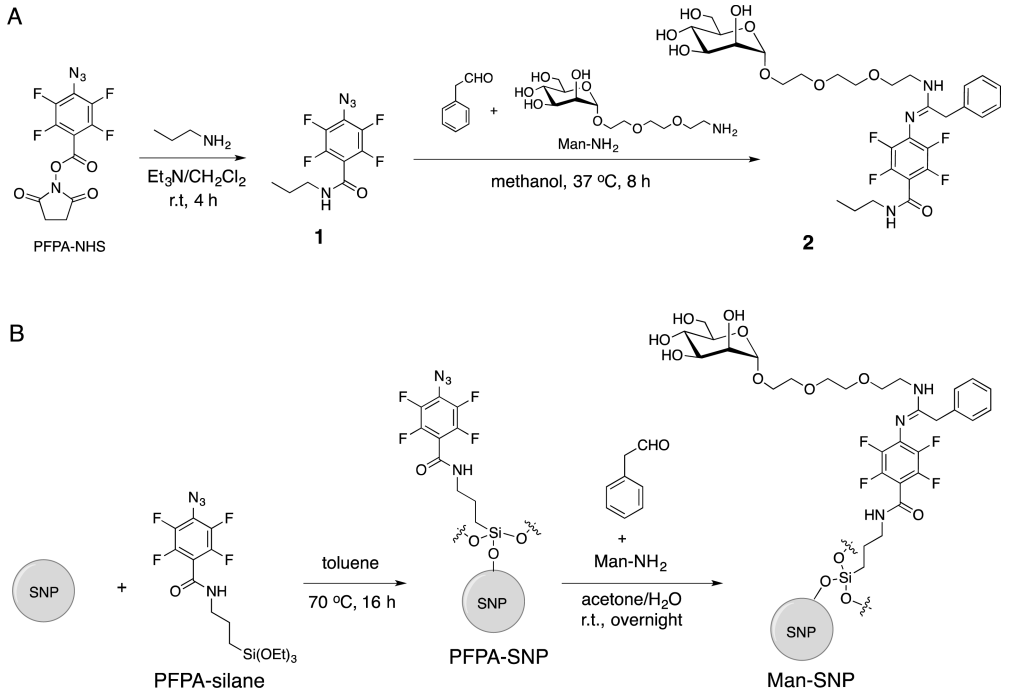

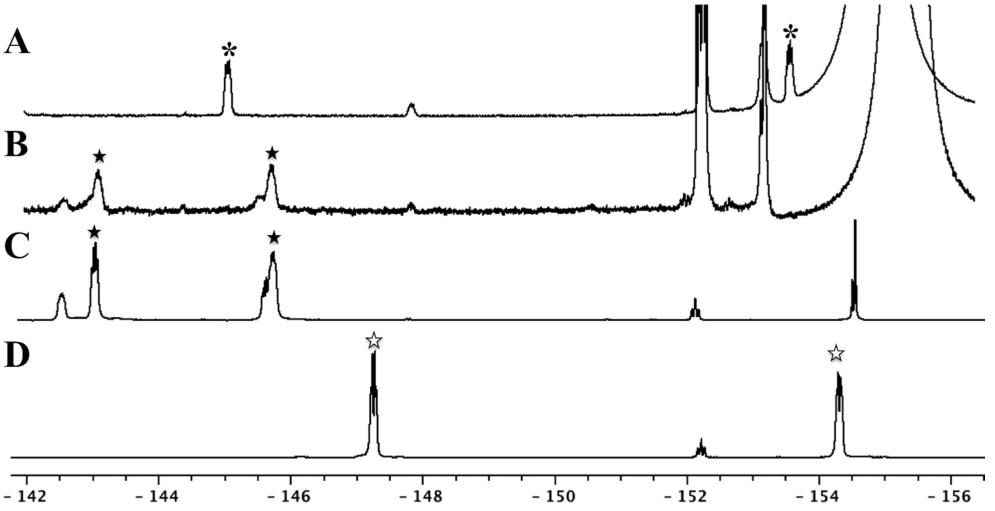

Figure 1. ^{19}F NMR spectra of (A) PFPA-SNPs, (B) Man-SNPs, and (C) model compound **2** after HF treatment, and (D) untreated model compound **2**, in methanol-d_4. The peak at 152.3 ppm, marked as "S" in all spectra, was from F-4 of the internal standard, methyl pentafluorobenzoate.

determine the carbohydrate density on the particles.[21] The binding affinity of the glyconanoparticles with lectin was evaluated by measuring the apparent dissociation constant (K_d) using a fluorescence competition assay. Isothermal titration calorimetry (ITC) was further applied to evaluate the influence of the coupling chemistry on lectin recognition in comparison to CuAAC.

RESULTS AND DISCUSSION

To test the feasibility of the perfluorophenyl azide-aldehyde-amine cycloaddition (AAAC) for carbohydrate conjugation, a model reaction was carried out by mixing 4-azido-*N*-butyl-2,3,5,6-tetrafluorobenzamide (**1**) with 2-[2-(2-aminoethoxy)-ethoxy]ethyl α-D-mannopyranoside (Man-NH_2) and phenylacetaldehyde in methanol-d_4 at 37 °C (Scheme 1A). The reaction proceeded by first forming an enamine from the Man-NH_2 and phenylacetaldehyde, followed by PFPA-enamine cycloaddition to give the triazoline, which spontaneously rearranges into the amidine product.[33] The reaction was monitored by ^{19}F NMR spectroscopy (Figure S1 of the Supporting Information). The product was formed after 8 h in 83% isolated yield (Figure S2 and Figure S3). This result demonstrates the feasibility of the three-component AAAC reaction for carbohydrate immobilization on nanoparticles.

Stöber SNPs of 87 ± 8 nm (Figure S4a) were prepared via NH_4OH-mediated hydrolysis and condensation of tetraethyl orthosilicate. A previously developed protocol was used to functionalize the SNPs using *N*-(3-triethoxysilylpropyl)-4-azidotetrafluorobenzoate (PFPA-silane) to give PFPA-functionalized SNP (PFPA-SNP, Scheme 1B).[37−39] The appearance of

DOI: 10.1021/acsami.6b07471
ACS Appl. Mater. Interfaces XXXX, XXX, XXX−XXX

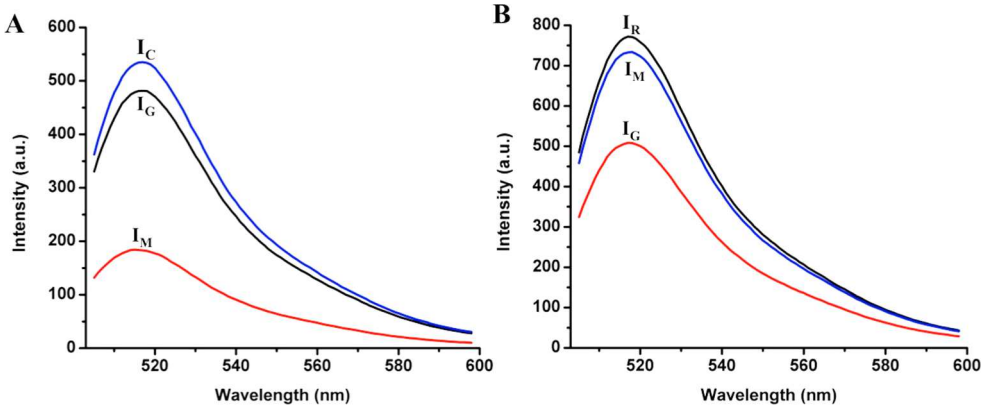

Figure 2. Fluorescence intensities of (A) FITC-Con A and (B) FITC-RCA I before (I_C and I_R) and after treating with Man-SNPs (I_M) and Gal-SNPs (I_G).

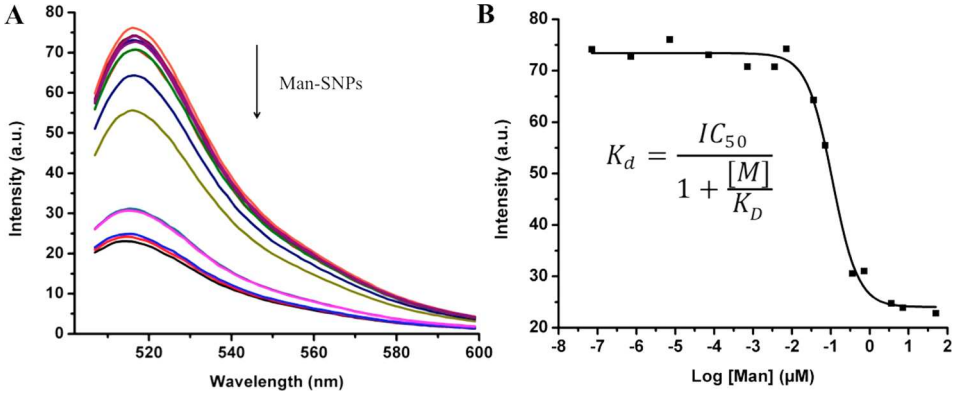

Figure 3. (A) Fluorescence spectra of the supernatant at different concentrations of Man-SNPs. FITC-Con A (380 nM) was incubated with Man (0.24 mM) and a concentration series of Man-SNPs (1×10^{-8} to 7 mg/mL) for 1 h, and centrifuged. The direction of the arrow indicates increasing concentration of Man-SNPs. (B) Fluorescence intensity of the supernatant vs log[Man] on Man-SNPs. Inset is the Cheng-Prusoff equation, where IC_{50} is the concentration of ligand displaying 50% of specific binding; K_D is the dissociation constant of Man with Con A; and K_d is the apparent dissociation constant of Man-SNPs with FITC-Con A.

the azide signal at 2134 cm^{-1} and the C═O absorption band at 1639 cm^{-1} in the FTIR spectrum of the PFPA-SNPs supported the conjugation of PFPA on the particles (Figure S5). The PFPA-SNPs were then mixed with phenylacetaldehyde in acetone, together with an aqueous solution of Man-NH_2, and stirred at room temperature overnight. Membrane dialysis followed by centrifugation gave the Man-presenting SNPs (Man-SNPs, Scheme 1B). The characteristic azide absorption on PFPA-SNPs disappeared after the reaction (Figure S5).

^{19}F qNMR, a method previously developed to determine the ligand density on glyconanoparticles prepared from PFPA-SNPs and the CuAAC reaction,[21] was used to determine the density of Man on Man-SNPs. Man-SNPs were treated with 5% aqueous HF under vigorous stirring at room temperature for 1 h, which dissolved SiO_2 and released the surface-bound ligands. The reaction mixture was subsequently lyophilized using an in-line CaO trap to remove the volatile components. The residues after lyophilization were subjected to ^{19}F NMR analysis in methanol-d_4 using methyl pentafluorobenzoate as the internal standard. Compared to PFPA-SNPs that had two sets of F peaks at −145.0 and −153.6 ppm (*, Figure 1A), two new sets of peaks at −142.8 ppm (★) and −145.7 ppm (★) were observed in Man-SNPs (Figure 1B). To aid the peak assignment, the model compound **2** was subjected to the same HF treatment. Two sets of F signals having the same chemical shifts (★, Figure 1C) as in Man-SNPs were observed. Interestingly, the signals shifted 4.5 ppm for F-2,6 and 8.6 ppm for F-3,5 from untreated compound **2** (☆, F-2,6 at −147.3 ppm and F-3,5 at −154.3 ppm, Figure 1D). The shifts might be due to the protonation of the amidine moiety under the acidic conditions. To test this hypothesis, the residues from Man-SNPs or compound **2** after HF treatment were titrated with triethylamine. Indeed, the F signals shifted after the addition of triethylamine, and the peaks matched those of untreated compound **2** (Figure S6). From these results, the two sets of peaks at −142.8 and −145.7 ppm from Man-SNPs (Figure 1B) were assigned to F-2,6 and F-3,5 of the PFPA moiety, respectively. Subsequently, the density of the Man ligands on Man-SNP was calculated to be $2.5 \pm 0.2 \times 10^{-16}$ nmol/nm^2 by comparing the integrals with that of F-4 on the internal standard of methyl pentafluorobenzoate (see Supporting Information for detailed calculations).

The binding properties of the synthesized glyconanoparticles were evaluated by interaction analyses with fluorescein (FITC)-labeled lectins: concanavalin A (Con A) and *Ricinus communis* agglutinin I (RCA I). Con A binds specifically to α-D-mannopyranosides,[40] and RCA I binds to β-D-galactopyranosides.[41] When Man-SNPs were incubated with FITC-Con A in phosphate buffered saline (PBS) for 1 h, the fluorescence intensity of the supernatant decreased significantly (I_M, Figure 2A), together with the formation of a sedimented solid. When the solid was examined under transmission electron microscopy

DOI: 10.1021/acsami.6b07471
ACS Appl. Mater. Interfaces XXXX, XXX, XXX−XXX

(TEM), large agglomerates were observed (Figure S7a). Galactose-presenting SNPs (Gal-SNPs) were synthesized following the same procedure as Man-SNPs, and were incubated with FITC-Con A. In this case, the fluorescence intensity of the supernatant decreased only slightly (I_G, Figure 2A), and the residual binding was likely due to the nonspecific protein absorption on the nanoparticles (Figure S7b). To further investigate the binding selectivity, the particles were treated with FITC-RCA I following an analogous procedure. The fluorescence intensity decreased after incubating with Gal-SNPs (I_G, Figure 2B), more than in the case of Man-SNPs (I_M, Figure 2B).

These binding patterns are consistent with the binding selectivity of the carbohydrates toward their cognate lectins. Furthermore, the lower degree of intensity decrease in the case of FITC-RCA I with Gal-SNPs in comparison to that of FITC-Con A with Man-SNPs was consistent with the lower binding affinity of Gal-RCA I (K_D = 833 μM)[42] compared to Man-Con A (K_D = 452 μM).[43] The particle agglomeration was due to the multivalent nature of the glyconanoparticles, as well as the tetrameric nature of Con A and RCA I (two As-sB-type dimers) at neutral pH. The lectin thus acted as a cross-linker when interacting with the glyconanoparticles, causing them to agglomerate.

A fluorescence competition assay was employed to quantitatively measure the binding affinity of the Man-SNPs with FITC-Con A.[21,44,45] A fixed concentration of the free Man ligand and a concentration series of Man-SNPs (1×10^{-8} to 7 mg/mL) were incubated with FITC-Con A. After incubation for 1 h, Man-SNPs, including those bound to FITC-Con A, were removed by centrifugation. The fluorescence intensity of the supernatant, which included the unbound FITC-Con A and the Man−Con A-FITC complex, was measured (Figure 3A). The IC_{50} value was obtained by analyzing the fluorescence intensity at 516 nm as a function of the logarithmic concentration of Man on Man-SNPs (Figure 3B). The apparent dissociation constant (K_d) of Man-SNPs with Con A was subsequently estimated to be 0.067 ± 0.005 μM (Figure 3B). Compared to that of free Man with Con A (K_D = 452 μM),[43] this represents 4 orders of magnitude enhancement of the binding affinity. The result was furthermore compared to that of Man-SNPs synthesized from PFPA-SNPs and an alkyne-derivatized mannose using the CuAAC click reaction.[21] The density of Man on the Man-SNPs prepared from the AAAC coupling chemistry was 2.6 times lower than that by CuAAC; however, the binding affinity of FITC-Con A with Man-SNPs synthesized by AAAC coupling was more than 4 times stronger than Man-SNPs synthesized by CuAAC (Table 1).

Several factors can affect the binding affinity of glyconanoparticles other than the ligand density, such as the coupling chemistry, linker type, and spacer length.[46] To evaluate these, the two model compounds synthesized by AAAC (**2**) and CuAAC (**2′**) together with methyl α-D-mannopyranoside (Manα1-OMe) were subjected to isothermal titration calorimetry (ITC) analysis. The data for the three compounds were fitted to the one set of sites model (Figure 4).

Table 1. Ligand Density and Binding Affinity of Con A with Man-SNPs Prepared from PFPA-SNPs Using AAAC or CuAAC Coupling Chemistry

coupling chemistry	size of SNPs (nm)	Man density on Man-SNP ($\times 10^{-16}$ nmol/nm^2)	K_d (μM)
AAAC	87 ± 8	2.5 ± 0.2	0.067 ± 0.005
CuAAC	87 ± 8	6.4 ± 0.2[21]	0.289 ± 0.003[21]

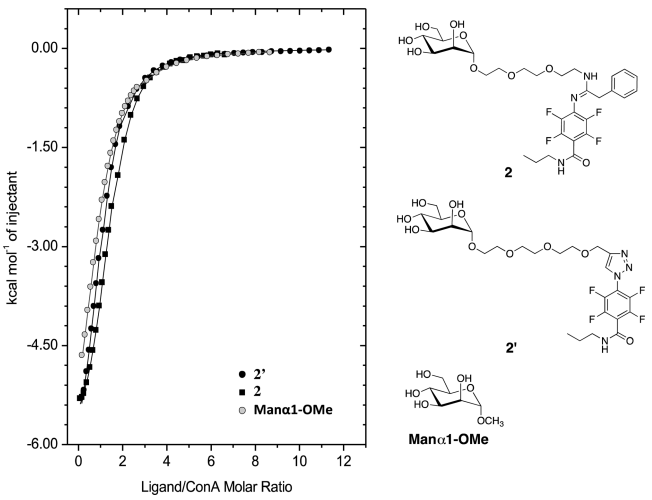

Figure 4. Calorimetric titration of Con A with Manα1-OMe (gray circles), compound **2** (black squares), and compound **2′** (black circles). Solid lines correspond to the best fit of the experimental data using the one set of sites model.

The thermodynamic parameters are shown in Table 2. Compound **2′**, similar to Manα1-OMe, bound to Con A with an almost 1:1 stoichiometry. For compound **2**, the ligand/protein ratio increased to 1.4, which could be due to self-association as some scattering of light was perceptible in the solutions, although no aggregation was observed. The slightly higher affinities of the two derivatives in comparison with Manα1-OMe also suggested that the interactions mediated by the substituents at position 1 could extend beyond the first methylene group, also supported by the enthalpic and entropic contributions to the binding. It can be noted that the recorded binding affinity of compound **2** is twofold higher than that of compound **2′**, in line with the higher affinity of Man-SNPs over those synthesized by CuAAC.

CONCLUSIONS

In conclusion, we have developed an efficient method to immobilize carbohydrates on nanoparticles using azide−aldehyde−amine cycloaddition reaction by simply mixing PFPA-SNPs, an amine-derivatized carbohydrate, and phenylacetaldehyde in a straightforward protocol under mild conditions without any catalyst. The density of Man on the Man-SNP was quantitatively determined using ^{19}F qNMR. The glyconanoparticles retained their binding affinity and selectivity toward cognate lectins, and the apparent dissociation constants were measured by a fluorescence competition assay. For example, the binding affinity of Man-SNPs was almost 4 orders of magnitude higher than that of Man with Con A. Moreover, even with a ligand density of 2.6 times lower than Man-SNPs synthesized by CuAAC, the binding affinity of Man-SNPs prepared by AAAC was more than 4 times higher. This result can be attributed to the higher affinity of the mannose derivative synthesized by AAAC than that synthesized by CuAAC, as supported by the ITC results. This new coupling chemistry avoids the use of a metal catalyst and results in the effective carbohydrate presentation. Since amine-containing compounds are ubiquitous in nature (e.g., proteins),

DOI: 10.1021/acsami.6b07471
ACS Appl. Mater. Interfaces XXXX, XXX, XXX−XXX

Table 2. Thermodynamic Parameters and K_d of Con A with Compound 2, Compound 2′, or Manα1-OMe Obtained by ITC

ligand	binding stoichiometry	K_d (μM)	ΔG (kcal/mol)	ΔH (kcal/mol)	$T\Delta S$(kcal/mol)
2	1.41 ± 0.01	44.5 ± 0.5	−5.92 ± 0.01	−6.34 ± 0.03	−0.42 ± 0.02
2′	1.07 ± 0.01	91.0 ± 2.0	−5.49 ± 0.01	−7.14 ± 0.05	−1.65 ± 0.02
Manα1-OMe	0.93 ± 0.01	121.5 ± 1.5	−5.317 ± 0.004	−7.62 ± 0.03	−2.30 ± 0.03

pharmaceuticals and synthetic polymers, this method extends beyond carbohydrates and offers a new way to prepare functional conjugates and nanomaterials.

EXPERIMENTAL PROCEDURES

Materials. PBS (0.01 M, pH 7.4) was prepared by dissolving PBS dry powder (containing TWEEN 20, Sigma-Aldrich, St. Louis) in deionized water. Fluorescein-labeled concanavalin A (FITC-Con A) and *Ricinus communis* Agglutinin I (FITC-RCA I) were purchased from Vector Laboratories (Burlingame, CA). All chemicals were used as received without purification. Water used was from a Milli-Q ultrapure water purification system. 2,5-Dioxopyrrolidin-1-yl 4-azido-2,3,5,6-tetrafluorobenzoate (PFPA-NHS)[47,48] and *N*-(3-triethoxysilylpropyl)-4-azidotetrafluorobenzoate (PFPA-silane)[49−51] were synthesized following previously reported procedures. 2-[2-(2-Aminoethoxy)ethoxy]ethyl α-D-mannopyranoside (Man-NH_2) and β-D-galactopyranoside (Gal-NH_2) were synthesized following previously established procedures.[52]

Instrumentation. ^{1}H-, ^{13}C-, and ^{19}F-NMR spectra were recorded on a Bruker DMX 500 instrument at 500 MHz (^{1}H) or 125 MHz (^{13}C), or on a Bruker Ascend 400 instrument at 400 MHz (^{1}H), 100 MHz (^{13}C), or 376 MHz (^{19}F) in $CDCl_3$, D_2O, or methanol-d_4. FTIR spectra were collected on a BioRad FTS375 spectrometer. Fluorescence measurements were conducted on a Varian Cary Eclipse fluorescence spectrophotometer (Agilent Technologies, Santa Clara, CA). Transmission electron microscopy (TEM) images were obtained on a JEOL 100CX transmission electron microscope operating at an accelerating bias voltage of 100 kV. Electrospray ionization high-resolution mass spectrometry (ESI-HRMS) data were obtained from Proteoomika tuumiklabor at the University of Tartu, Estonia. ITC was performed at 25 °C with a Microcal VP-ITC microcalorimeter (GE Healthcare, Little Chalfont, U.K.).

Synthesis of 4-Azido-*N*-butyl-2,3,5,6-tetrafluorobenzamide (1). PFPA-NHS (100 mg, 0.30 mmol), triethylamine (30 mg, 0.30 mmol), and propylamine (19 mg, 0.32 mmol) were dissolved in dichloromethane (15 mL), and the solution was stirred at room temperature for 4 h. The resulting mixture was diluted with water and extracted twice with dichloromethane. The combined organic phase was washed with 1 M HCl, followed by brine. After drying over $MgSO_4$ and evaporation of the solvent under reduced pressure, the crude product was purified by flash column chromatography using hexanes/EtOAc (3:1, v/v) to yield compound **1** as white crystals (69 mg, 83%). ^{1}H NMR (400 MHz, methanol-d_4): δ 3.35 (m, 2 H, $NHCH_2$), δ 1.63 (m, 2 H, CH_3CH_2), 0.91 (t, 3H, J = 7.17 Hz, CH_2CH_3). ^{13}C NMR (100 MHz, methanol-d_4): δ 160.1, 146.6, 143.9, 143.4, 110.4, 42.8, 23.4, 11.6. ^{19}F NMR (376 MHz, methanol-d_4): δ 145.0, 153.6.

Model Compound 2. Compound **1** (15 mg, 0.055 mmol), phenylacetaldehyde (17 mg, 0.14 mmol), and Man-NH_2 (25 mg, 0.083 mmol) were dissolved in methanol-d_4 (1.5 mL). The mixture was stirred at 37 °C for 8 h, after which ^{19}F NMR showed a conversion of 91%. The crude product was purified by flash column chromatography using CH_2Cl_2/methanol (7:1, v/v) to give compound **2** as a yellow oil (30 mg, 83%). ^{1}H NMR (400 MHz, methanol-d_4): δ 7.3−7.02 (m, 5 H, CH_5), 4.80 (s, 1 H, H-1), 3.86−3.50 (m, 18 H, 5 × OCH_2, CCH_2, H-2, H-3, H-4, H-5, H-6a, 6b), 3.21 (dd, J = 7.32 and 14.5 Hz, 4 H, 2 × $NHCH_2$), δ 1.62 (m, 2 H, $NHCH_2CH_2$), 0.98 (t, 3H, J = 7.34 Hz, CH_2CH_3). ^{13}C NMR (100 MHz, methanol-d_4): δ 163.2, 161.4, 136.2, 129.6, 127.9, 101.8, 74.6,72.6, 72.1, 71.6, 71.4, 71.3, 69.8, 68.6, 67.7, 62.9, 42.7, 42.4, 30.7, 23.4, 11.6. ^{19}F NMR (376 MHz, methanol-d_4): δ 147.3, 154.3. ESI-HRMS: Calcd for $C_{30}H_{39}F_4N_3O_9$ $[M + H]^+$: 662.2695, obtained 662.2700. FTIR: 628.3, 676.4, 703.4, 748.6, 811.6, 895.6, 976.7, 1030.8, 1063.8, 1093.8, 1132.9, 1217.1, 1229.2, 1364.4, 1442.5, 1475.5, 1531.4, 1545.9, 1598.7, 1615.5, 1656.4, 1740.5, 2869.6, 2941.6, 2971.8, 3019.9, 3085.9, 3356.2 cm^{-1}.

Synthesis of PFPA-Functionalized SNPs. Silica nanoparticles were synthesized following a previous protocol.[21,53] PFPA-silane (219 mg, 0.5 mmol) was added into a suspension of SNPs (400 mg) in dry toluene (10 mL), and the mixture was stirred at 70 °C for 16 h. The resulting nanoparticles were isolated by centrifugation and washed with toluene (7500 rpm, two times) and ethanol (7500 rpm, two times). The obtained PFPA-SNPs were dried under vacuum.

Conjugation of Carbohydrates. To an acetone solution (6 mL) of PFPA-SNPs (70 mg) and phenylacetaldehyde (96 mg, 0.8 mmol), an aqueous solution (1.5 mL) of Man-NH_2 or Gal-NH_2 (250 mg, 0.8 mmol) was added. The mixture was stirred at room temperature overnight. Centrifugation of the mixture at 11 000 rpm for 15 min separated the nanoparticles as a sedimented solid. Excess reagents were removed by membrane dialysis (MW cutoff: 12 000−14 000 Da) in water for 5 h. The solid was then washed with water (11 000 rpm, two times) and acetone (11 000 rpm, three times). The solid was finally dried under reduced pressure to give Man- or Gal-SNPs (53 mg).

TEM Analysis. Samples for the TEM measurement were prepared by dropping the suspension of SNPs in ethanol or glyco-SNPs−lectin complexes in water onto a Cu grid (200 mesh), and vacuum drying for a few hours. The particle size was estimated by averaging the diameters of >100 nanoparticles.

Determination of Man Density on Man-SNPs. Man-SNPs (50 mg) were treated with 5% HF aqueous solution (3 mL) at room temperature for 1 h under vigorous stirring. The resulting solution was subsequently lyophilized to remove the volatile components by an in-line trap containing CaO. The obtained products were subjected to ^{19}F NMR analysis in methanol-d_4. Methyl pentafluorobenzoate (1.5 mg, 0.0066 mmol) was added as the internal standard.

Binding of Glyconanoparticles with Lectins. Man-SNPs or Gal-SNPs (3.0 mg) were incubated in a solution of BSA (3 wt %) in pH 7.4 PBS buffer containing 0.05% Tween (2.0 mL, 10 mM) for 30 min, and centrifuged. The sediment was then incubated in a pH 7.4 PBS buffer containing 0.05% Tween for another 20 min and centrifuged. The resulting Man-SNPs or Gal-SNPs were subsequently incubated with a solution of FITC-Con A (2.5 mL, 10 μg/mL) containing $MnCl_2$ (1.0 mM) and $CaCl_2$ (1.0 mM), or FITC-RCA I (2.5 mL, 10 μg/mL) in pH 7.4 PBS buffer under ambient conditions for 1 h while shaking. The mixture was centrifuged to separate the unbound FITC-Con A and FITC-RCA I. The fluorescence intensity of the supernatant was measured using a spectrofluorimeter.

Fluorescence Competition Binding Assay. Solutions of FITC-Con A (380 nM), Man (2.88 mM), and a concentration series of Man-SNPs (1×10^{-8} to 7 mg/mL) were prepared in pH 7.4 PBS buffer containing $MnCl_2$ (1 mM) and $CaCl_2$ (1 mM). To Man-SNPs (1 mL) in 1.5 mL microcentrifuge tubes, Man (2.88 mM, 0.1 mL) and FITC-Con A (380 nM, 0.1 mL) were added. The mixtures were shaken for 1 h and centrifuged at 10 500 rpm for 20 min. The fluorescence emission of the supernatant at 516 nm was recorded. The measurement at each concentration was repeated three times, and the mean value of the emission intensities was used for the analysis.

ITC Analysis. Con A was exhaustively dialyzed against PBS (pH 7.4) supplemented with 1 mM $CaCl_2$, and ligand solutions were prepared in the final dialysate. The protein concentration was determined spectrophotometrically at 280 nm (monomer molar extinction coefficient 31 741 outside diameter cm^{-1} M^{-1}). Titrations were performed by stepwise injections of the ligand (7.6−16 mM) into the reaction cell loaded with Con A (189−296 μM). The heat of

DOI: 10.1021/acsami.6b07471
ACS Appl. Mater. Interfaces XXXX, XXX, XXX−XXX

ligand dilution was determined separately and was subtracted from the total heat produced following each injection. Titration data were analyzed with the ORIGIN software (GE Healthcare) using Con A monomer concentration as input in the fitting procedure.

■ ASSOCIATED CONTENT

Supporting Information

The Supporting Information is available free of charge on the ACS Publications website at DOI: 10.1021/acsami.6b07471.

Additional data and control experiments, and carbohydrate density calculation (PDF)

■ AUTHOR INFORMATION

Corresponding Authors

*E-mail: ramstrom@kth.se (O.R.).

*E-mail: mingdi@kth.se (M.Y.).

Notes

The authors declare no competing financial interest.

■ ACKNOWLEDGMENTS

This work was in part supported by the National Institutes of Health (R01GM080295, to M.Y.), the National Science Foundation (CHE-1112436, to M.Y.), KTH, the Marie Curie Initial Training Network DYNANO (PITN-GA-2011-289033), the CIBER of Respiratory Diseases (CIBERES), an initiative from the Spanish Institute of Health Carlos III (ISCIII), and the Spanish Ministry of Economy and Competitiveness (BFU2012-36825). N.K., S.X., and J.Z. thank the China Scholarship Council for special scholarship awards.

■ REFERENCES

(1) Chen, X.; Ramström, O.; Yan, M. Glyconanomaterials: Emerging Applications in Biomedical Research. *Nano Res.* **2014**, *7*, 1381−1403.

(2) Hao, N.; Neranon, K.; Ramström, O.; Yan, M. Glyconanomaterials for Biosensing Applications. *Biosens. Bioelectron.* **2016**, *76*, 113−130.

(3) Solís, D.; Bovin, N. V.; Davis, A. P.; Jiménez-Barbero, J.; Romero, A.; Roy, R.; Smetana, K., Jr; Gabius, H-J. A Guide into Glycosciences: How Chemistry, Biochemistry and Biology Cooperate to Crack the Sugar Code. *Biochim. Biophys. Acta, Gen. Subj.* **2015**, *1850*, 186−235.

(4) Wang, Y.; Qu, K.; Tang, L.; Li, Z.; Moore, E.; Zeng, X.; Liu, Y.; Li, J. Nanomaterials in Carbohydrate Biosensors. *TrAC, Trends Anal. Chem.* **2014**, *58*, 54−70.

(5) Kennedy, D. C.; Grünstein, D.; Lai, C.-H.; Seeberger, P. H. Glycosylated Nanoscale Surfaces: Preparation and Applications in Medicine and Molecular Biology. *Chem. - Eur. J.* **2013**, *19*, 3794−3800.

(6) Adak, A. K.; Lin, H. J.; Lin, C. C. Multivalent Glycosylated Nanoparticles for Studying Carbohydrate-Protein Interactions. *Org. Biomol. Chem.* **2014**, *12*, 5563−5573.

(7) El-Boubbou, K.; Huang, X. Glyco-Nanomaterials: Translating Insights from the "Sugar-Code" to Biomedical Applications. *Curr. Med. Chem.* **2011**, *18*, 2060−2078.

(8) Wang, X.; Liu, L. H.; Ramström, O.; Yan, M. Engineering Nanomaterial Surfaces for Biomedical Applications. *Exp. Biol. Med.* **2009**, *234*, 1128−1139.

(9) Ramström, O.; Yan, M. Glyconanomaterials for Combating Bacterial Infections. *Chem. - Eur. J.* **2015**, *21*, 16310−16317.

(10) Jayawardena, H. S. N.; Jayawardana, K. W.; Chen, X.; Yan, M. Maltoheptaose Promotes Nanoparticle Internalization by Escherichia Coli. *Chem. Commun.* **2013**, *49*, 3034−3036.

(11) Jayawardana, K. W.; Wijesundera, S. A.; Yan, M. Aggregation-Based Detection of M. Smegmatis Using D-Arabinose-Functionalized Fluorescent Silica Nanoparticles. *Chem. Commun.* **2015**, *51*, 15964−15966.

(12) Jayawardana, K. W.; Jayawardena, H. S. N.; Wijesundera, S. A.; De Zoysa, T.; Sundhoro, M.; Yan, M. Selective Targeting of Mycobacterium Smegmatis with Trehalose-Functionalized Nanoparticles. *Chem. Commun.* **2015**, *51*, 12028−12031.

(13) Hao, N.; Jayawardana, K. W.; Chen, X.; Yan, M. One-Step Synthesis of Amine-Functionalized Hollow Mesoporous Silica Nanoparticles as Efficient Antibacterial and Anticancer Materials. *ACS Appl. Mater. Interfaces* **2015**, *7*, 1040−1045.

(14) Zhou, J.; Hao, N.; De Zoyza, T.; Yan, M.; Ramström, O. Lectin-Gated, Mesoporous, Photofunctionalized Glyconanoparticles for Glutathione-Responsive Drug Delivery. *Chem. Commun.* **2015**, *51*, 9833−9836.

(15) Hao, N.; Chen, X.; Jeon, S.; Yan, M. Carbohydrate-Conjugated Hollow Oblate Mesoporous Silica Nanoparticles as Nanoantibiotics to Target Mycobacteria. *Adv. Healthcare Mater.* **2015**, *4*, 2797−2801.

(16) Wang, X.; Ramström, O.; Yan, M. Glyconanomaterials: Synthesis, Characterization, and Ligand Presentation. *Adv. Mater.* **2010**, *22*, 1946−1953.

(17) Santoyo-Gonzalez, F.; Hernandez-Mateo, F. Silica-Based Clicked Hybrid Glyco Materials. *Chem. Soc. Rev.* **2009**, *38*, 3449−3462.

(18) Lutz, J.-F.; Zarafshani, Z. Efficient Construction of Therapeutics, Bioconjugates, Biomaterials and Bioactive Surfaces Using Azide−Alkyne "Click" Chemistry. *Adv. Drug Delivery Rev.* **2008**, *60*, 958−970.

(19) Pieters, R. J.; Rijkers, D. T. S.; Liskamp, R M J. Application of the 1,3-Dipolar Cycloaddition Reaction in Chemical Biology: Approaches toward Multivalent Carbohydrates and Peptides and Peptide-Based Polymers. *QSAR Comb. Sci.* **2007**, *26*, 1181−1190.

(20) Kushwaha, D.; Dwivedi, P.; Kuanar, S. K.; Tiwari, V. K. Click Reaction in Carbohydrate Chemistry: Recent Developments and Future Perspective. *Curr. Org. Synth.* **2013**, *10*, 90−135.

(21) Kong, N.; Zhou, J.; Park, J.; Xie, S.; Ramström, O.; Yan, M. Quantitative Fluorine NMR to Determine Carbohydrate Density on Glyconanomaterials Synthesized from Perfluorophenyl Azide-Functionalized Silica Nanoparticles by Click Reaction. *Anal. Chem.* **2015**, *87*, 9451−9458.

(22) Hou, Y.; Cao, S.; Li, X.; Wang, B.; Pei, Y.; Wang, L.; Pei, Z. One-Step Synthesis of Dual Clickable Nanospheres Via Ultrasonic-Assisted Click Polymerization for Biological Applications. *ACS Appl. Mater. Interfaces* **2014**, *6*, 16909−16917.

(23) Hu, X.-L.; Zang, Y.; Li, J.; Chen, G.-R.; James, T. D.; He, X.-P.; Tian, H. Targeted Multimodal Theranostics Via Biorecognition Controlled Aggregation of Metallic Nanoparticle Composites. *Chem. Sci.* **2016**, *7*, 4004−4008.

(24) Lallana, E.; Fernandez-Megia, E.; Riguera, R. Surpassing the Use of Copper in the Click Functionalization of Polymeric Nanostructures: A Strain-Promoted Approach. *J. Am. Chem. Soc.* **2009**, *131*, 5748−5750.

(25) Hu, X.-L.; Jin, H.-Y.; He, X.-P.; James, T. D.; Chen, G.-R.; Long, Y.-T. Colorimetric and Plasmonic Detection of Lectins Using Core−Shell Gold Glyconanoparticles Prepared by Copper-Free Click Chemistry. *ACS Appl. Mater. Interfaces* **2015**, *7*, 1874−1878.

(26) He, X.-P.; Hu, X.-L.; Jin, H.-Y.; Gan, J.; Zhu, H.; Li, J.; Long, Y.-T.; Tian, H. Quick Serological Detection of a Cancer Biomarker with an Agglutinated Supramolecular Glycoprobe. *Anal. Chem.* **2015**, *87*, 9078−9083.

(27) Zhang, H.; Ma, Y.; Sun, X.-L. Chemically-Selective Surface Glyco-Functionalization of Liposomes through Staudinger Ligation. *Chem. Commun.* **2009**, 3032−3034.

(28) Yang, M.; Li, J.; Chen, P. R. Transition Metal-Mediated Bioorthogonal Protein Chemistry in Living Cells. *Chem. Soc. Rev.* **2014**, *43*, 6511−6526.

(29) Zhang, Z.; Dong, C.; Yang, C.; Hu, D.; Long, J.; Wang, L.; Li, H.; Chen, Y.; Kong, D. Stabilized Copper(I) Oxide Nanoparticles Catalyze Azide-Alkyne Click Reactions in Water. *Adv. Synth. Catal.* **2010**, *352*, 1600−1604.

(30) Wang, Q.; Chan, T. R.; Hilgraf, R.; Fokin, V. V.; Sharpless, K. B.; Finn, M. G. Bioconjugation by Copper(I)-Catalyzed Azide-Alkyne [3 + 2] Cycloaddition. *J. Am. Chem. Soc.* **2003**, *125*, 3192−3193.

DOI: 10.1021/acsami.6b07471
ACS Appl. Mater. Interfaces XXXX, XXX, XXX−XXX

(31) Lutz, J.-F. Copper-Free Azide−Alkyne Cycloadditions: New Insights and Perspectives. *Angew. Chem., Int. Ed.* **2008**, *47*, 2182−2184.
(32) Zhang, X.; Zhang, Y. Applications of Azide-Based Bioorthogonal Click Chemistry in Glycobiology. *Molecules* **2013**, *18*, 7145−7159.
(33) Xie, S.; Lopez, S. A.; Ramström, O.; Yan, M.; Houk, K. N. 1,3-Dipolar Cycloaddition Reactivities of Perfluorinated Aryl Azides with Enamines and Strained Dipolarophiles. *J. Am. Chem. Soc.* **2015**, *137*, 2958−2966.
(34) Xie, S.; Ramström, O.; Yan, M. N. N-Diethylurea-Catalyzed Amidation between Electron-Deficient Aryl Azides and Phenylacetaldehydes. *Org. Lett.* **2015**, *17*, 636−639.
(35) Xie, S.; Fukumoto, R.; Ramström, O.; Yan, M. Anilide Formation from Thioacids and Perfluoroaryl Azides. *J. Org. Chem.* **2015**, *80*, 4392−4397.
(36) Xie, S.; Zhang, Y.; Ramström, O.; Yan, M. Base-Catalyzed Synthesis of Aryl Amides from Aryl Azides and Aldehydes. *Chem. Sci.* **2016**, *7*, 713−718.
(37) Gann, J. P.; Yan, M. A Versatile Method for Grafting Polymers on Nanoparticles. *Langmuir* **2008**, *24*, 5319−5323.
(38) Wang, X.; Ramström, O.; Yan, M. Dynamic Light Scattering as an Efficient Tool to Study Glyconanoparticle-Lectin Interactions. *Analyst* **2011**, *136*, 4174−4178.
(39) Wang, X.; Ramström, O.; Yan, M. Dye-Doped Silica Nanoparticles as Efficient Labels for Glycans. *Chem. Commun.* **2011**, *47*, 4261−4263.
(40) Becker, J. W.; Reeke, G. N.; Wang, J. L.; Cunningham, B. A.; Edelman, G. M. The Covalent and Three-Dimensional Structure of Concanavalin A. III. Structure of the Monomer and Its Interactions with Metals and Saccharides. *J. Biol. Chem.* **1975**, *250*, 1513−1524.
(41) Wu, A. M.; Wu, J. H.; Singh, T.; Lai, L.-J.; Yang, Z.; Herp, A. Recognition Factors of Ricinus Communis Agglutinin 1 (Rca1). *Mol. Immunol.* **2006**, *43*, 1700−1715.
(42) Podder, S. K.; Surolia, A.; Bachhawat, B. K. On the Specificity of Carbohydrate-Lectin Recognition. *Eur. J. Biochem.* **1974**, *44*, 151−160.
(43) Schwarz, F. P.; Puri, K. D.; Bhat, R. G.; Surolia, A. Thermodynamics of Monosaccharide Binding to Concanavalin a, Pea (Pisum Sativum) Lectin, and Lentil (Lens Culinaris) Lectin. *J. Biol. Chem.* **1993**, *268*, 7668−7677.
(44) Wang, X.; Matei, E.; Deng, L.; Ramström, O.; Gronenborn, A. M.; Yan, M. Multivalent Glyconanoparticles with Enhanced Affinity to the Anti-Viral Lectin Cyanovirin-N. *Chem. Commun.* **2011**, *47*, 8620−8622.
(45) Wang, X.; Matei, E.; Deng, L.; Koharudin, L.; Gronenborn, A. M.; Ramström, O.; Yan, M. Sensing Lectin−Glycan Interactions Using Lectin Super-Microarrays and Glycans Labeled with Dye-Doped Silica Nanoparticles. *Biosens. Bioelectron.* **2013**, *47*, 258−264.
(46) Wang, X.; Ramström; Yan, M. Quantitative Analysis of Multivalent Ligand Presentation on Gold Glyconanoparticles and the Impact on Lectin Binding. *Anal. Chem.* **2010**, *82*, 9082−9089.
(47) Norberg, O.; Deng, L.; Yan, M.; Ramström, O. Photo-Click Immobilization of Carbohydrates on Polymeric Surfaces—a Quick Method to Functionalize Surfaces for Biomolecular Recognition Studies. *Bioconjugate Chem.* **2009**, *20*, 2364−2370.
(48) Norberg, O.; Deng, L.; Aastrup, T.; Yan, M.; Ramström, O. Photo-Click Immobilization on Quartz Crystal Microbalance Sensors for Selective Carbohydrate−Protein Interaction Analyses. *Anal. Chem.* **2011**, *83*, 1000−1007.
(49) Liu, L.; Yan, M. A General Approach to the Covalent Immobilization of Single Polymers. *Angew. Chem.* **2006**, *118*, 6353−6356.
(50) Wang, X.; Matei, E.; Gronenborn, A. M.; Ramström, O.; Yan, M. Direct Measurement of Glyconanoparticles and Lectin Interactions by Isothermal Titration Calorimetry. *Anal. Chem.* **2012**, *84*, 4248−4252.
(51) Wang, H.; Li, L.; Tong, Q.; Yan, M. Evaluation of Photochemically Immobilized Poly(2-Ethyl-2-Oxazoline) Thin Films as Protein-Resistant Surfaces. *ACS Appl. Mater. Interfaces* **2011**, *3*, 3463−3471.
(52) Kong, N.; Shimpi, M. R.; Ramström, O.; Yan, M. Carbohydrate Conjugation through Microwave-Assisted Functionalization of Single-Walled Carbon Nanotubes Using Perfluorophenyl Azides. *Carbohydr. Res.* **2015**, *405*, 33−38.
(53) Park, J.; Jayawardena, H. S. N.; Chen, X.; Jayawardana, K. W.; Sundhoro, M.; Ada, E.; Yan, M. A General Method for the Fabrication of Graphene-Nanoparticle Hybrid Material. *Chem. Commun.* **2015**, *51*, 2882−2885.

DOI: 10.1021/acsami.6b07471
ACS Appl. Mater. Interfaces XXXX, XXX, XXX−XXX